# Interfacial electronic properties of pentacene tuned by a molecular monolayer of $C_{60}$

X. Liu, Y. Zhan, S. Braun, F. Li, and M. Fahlman
*Department of Physics, Chemistry and Biology, Linköping University, S-581 83 Linköping, Sweden*
(Received 23 April 2009; revised manuscript received 9 July 2009; published 1 September 2009)

Fine-tuning charge injection barriers between organic materials and electrodes is critical to optimize organic electronic device performance. Here we demonstrate that by modifying gold substrates with a monolayer of fullerene, significant decrease in the hole-injection barrier into pentacene films can be achieved. The insertion of the fullerene monolayer modifies the interfacial dipole and produces an interface where the pentacene molecules form a standing-up orientation with their long axis parallel to the surface normal. The latter effect lowers the vertical ionization energy of the pentacene molecules at the interface as compared to the pentacene-on-Au case, as well as improves the $\pi-\pi$ overlap between the pentacene molecules that will likely enhance the transport properties in corresponding devices.

DOI: 10.1103/PhysRevB.80.115401 PACS number(s): 73.20.−r, 71.20.Rv, 79.60.Dp, 78.70.Dm

## I. INTRODUCTION

Currently, organic semiconducting materials have attracted much attention due to their unique properties in the prospective applications in organic electronics such as light-emitting diodes, photovoltaic cells, and field effect transistors.[1–3] Functionalities of these devices are often determined to a large extent by the energy-level alignment at the various metal-organic and organic-organic interfaces. Processes such as, e.g., charge injection as well as exciton formation, dissociation, and recombination are strongly dependent on the interface energetics.[4–6] Therefore, the energy-level alignment at heterojunctions is a key property in the process of designing organic electronic devices. Unfortunately, energy-level diagrams often cannot be obtained merely by using the values of ionization potential, electron affinity, and work function of the materials involved, due to complex interactions at the interfaces.[7–9] For example, deposition of organic semiconductors onto metal surfaces often results in dipole formation at the interfacial region.[7–18] The interaction strength at an interface generally determines which type of processes dominate in determining the energetics and hence which type of regime, vacuum level alignment,[19] or interface dipole induced off-set of the vacuum level is observed.[7] For the weakly interacting (physisorption) case, i.e., organic-organic interfaces or organic-metal interfaces where the metal surface is passivated by, e.g., an oxide, hydrocarbon contaminants, or a dipole-inducing molecular adsorbant, the so-called integer charge-transfer (ICT) model can be applied.[8,14,20–22] In the case of interfaces with moderate chemical interactions, an induced density of interface states (IDIS) model can be applied. The IDIS model describes the interfaces formed by vapor deposition of $\pi$-conjugated molecules on clean but nonreactive metals such as gold, as has been used to model interfaces of organic molecules adsorbed on self-assembled monolayer modified metal systems.[9,23,24] In the ICT model, the key input parameters are the substrate work function, $\Phi_{SUB}$, as well as energies of the positive integer charge-transfer state, $E_{ICT+}$, and the negative integer charge-transfer state, $E_{ICT-}$, of the deposited organic film. The presence of a passivating overlayer (oxide, hydrocarbon, molecular adsorbant) modifies the work function of a metal substrate through the push-back effect, and some molecules will further modify the work function due to the charge-transfer effects, intrinsic dipoles, etc. Hence the resulting "effective" work function of the metal must be used as $\Phi_{SUB}$ rather than the work function of the clean metal surface.[8,14,25] Care must be also taken when using the $E_{ICT+}$ and $E_{ICT-}$ values, as they represent energies of the integer charge-transfer states of the molecules/polymers at the interface that may differ from the values in the bulk film, and may be affected as well by order/disorder in the layer(s) adjacent to the substrate.[8,14] Molecular order/disorder at the interface also is important in the context of energy-level alignment in the strongly interacting (chemisorption) regimes, as shown in series of recent articles.[26–28] Furthermore, these studies report dependence of molecular orientation on the value of ionization energy, which, in turn modifies charge injection barriers. Engineering the interface energy-level alignment through the use of thin insulating barrier layers[29–32] and dipole-inducing molecular adsorbants[33–37] are consequently quite complex, particularly in the case of molecular films, as the barrier layer or dipole-inducing molecular adsorbant may affect the order in the subsequent molecular overlayer and hence the interface energetics. We illustrate this general point for charge injecting/separating interfaces in organic electronic devices by using pentacene thin films deposited on gold and $C_{60}$-modified gold substrates, as pentacene films on $SiO_x$ have been demonstrated to have large difference in the vertical ionization potential ($\Delta IP=0.55$ eV) depending on the orientation of the pentacene molecules,[28] whereas the symmetry of the $C_{60}$ molecule prevents it from undergoing this effect.

Our choice of material systems is also guided by the great interest in pentacene and fullerene $C_{60}$ for use in organic electronic devices. Part of that interest is based on their high field-effect hole and electron mobility, respectively.[38,39] Furthermore, the absorption peak in pentacene is located close to the maximum of the solar visible spectra, making a bipolar pentacene $C_{60}$ diode promising for solar cell application.[40] The growth process of pentacene films can exhibit thickness-dependent competitive growth between a thin-film phase of pentacene with standing-up orientation and a phase with lying-down orientation.[41] The corresponding interface prop-

 

erties are strongly influenced by the film morphology, which in turn influences the device performance dependent on charge-carrier transport across the interface. For example, the reported values of the hole-injection barrier for pentacene/polycrystalline gold interfaces vary from 0.5 to 1.0 eV,[42–45] likely an effect of different molecular order at the pentacene/Au interface in the respective devices. Obviously, in order to maximize efficiency and device performance with high reproducibility, pentacene films with uniform growth and optimized order should be realized.

## II. EXPERIMENTAL

Photoemission experiments were carried out using a Scienta® ESCA 200 spectrometer in ultrahigh vacuum with a base pressure of $1\times10^{-10}$ mbar. The measurement chamber is equipped with a monochromatic Al($K\alpha$) x-ray source and He discharged lamp providing photons with 1486.6 eV for XPS (x-ray photoemission spectroscopy) and 21.22 eV for UPS (ultraviolet photoemission spectroscopy), respectively. The XPS experimental condition was set so that the full width at half maximum of the clean Au $4f_{7/2}$ line was 0.65 eV. The total-energy resolution of the measurements in UPS, determined by Fermi edge of clean gold, is about 0.1 eV. All spectra were measured at a photoelectron takeoff angle of 0° (normal emission). The UPS spectra have been corrected for the contributions from He I satellites radiation. The work-functions $\Phi$ of the films were extracted from the determination of the high binding-energy cutoff of the UPS spectra by applying a bias of −3 V to the sample.

Polarized x-ray absorption spectroscopy measurements were performed at beam line D1011 of the MAX-II storage ring, located at the MAX-Laboratory for Synchrotron Radiation Research in Lund, Sweden. The energy resolution was about 100 meV at photon energy close to the C *K* edge. The adsorption spectrum was collected in the total electron yield mode by measuring the sample current. The raw data have been corrected for the energy dependence of the incident x-ray beam and subsequently normalized to have the same absorption edge step well above threshold.

Thin films of pentacene (99.9% Syncom BV) with different thicknesses were prepared on a sputter-cleaned polycrystalline gold foil by *in situ* vacuum evaporation in a preparation chamber (base pressure $2\times10^{-10}$ mbar) with an evaporation rate of 1–2 Å/min from a Knudsen-type organic evaporator. We have chosen polycrystalline gold as substrate in order to simulate conditions often found in device applications. Subsequently, the films were transferred to the measurement chamber. Careful attention has been paid to the effects of charging and radiation damage and we can exclude any impact of those on our results. The thickness of the respective pentacene layer was estimated by monitoring the attenuation of the intensity of the core-level signals of the bottom layer (i.e., Au $4f_{7/2}$) due to the organic overlayer deposition.[46,47] In order to quantify the film thicknesses we used an estimation of the electron mean-free path according to Seah and Dench.[47] We point out that this procedure to determine the film thickness is only correct for a layer by layer growth of the organic film. If the organic film is not uniform, this method underestimates the film thickness. We estimate the error of film thickness determination to be on the order of 20%.

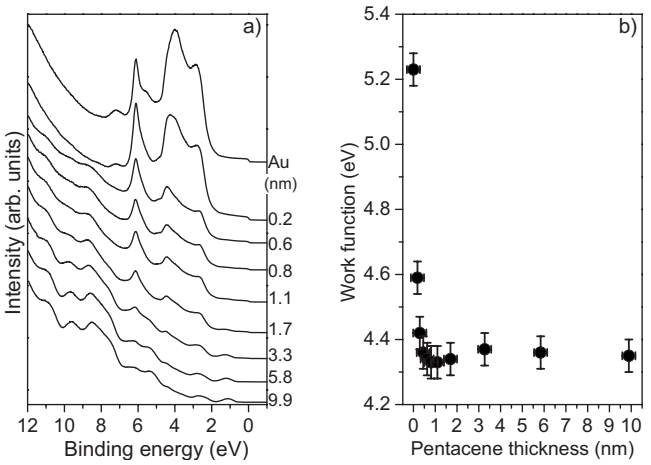


FIG. 1. (a) UPS spectra for increasing thickness of pentacene on Au. The labels indicate the corresponding pentacene film thickness (nm). (b) Dependence of the work function upon pentacene thickness obtained from UPS measurements.

To prepare a monolayer of $C_{60}$ (99.9% MER Tucson) on polycrystalline gold, a well-accepted preparation recipe was used,[48,49] first thick $C_{60}$ film (about 4–5 nm) was deposited on substrate, then the film was annealed at 300 °C for 20 min. Due to stronger interaction between $C_{60}$ and substrate than $C_{60}$ multilayer, the annealing finally generates a uniform $C_{60}$ monolayer. The monolayer $C_{60}$ thickness is about 0.8 nm estimated from the attenuation of the intensity of the core-level signals of the bottom layer, which is in a good agreement with published data.[50]

## III. RESULTS AND DISCUSSION

### A. Pentacene-on-Au foil

Figure 1(a) shows the UPS spectra of vapor-deposited pentacene-on-Au foil during the step-by-step evaporation. As the thickness of pentacene film increases the initial spectral feature of Au becomes weaker, and transforms into that of pentacene. Due to the strong valence-band feature from the Au substrate, the HOMO (highest occupied molecular orbital) level of the pentacene, at the early stage of the pentacene film deposition, cannot be fully resolved, but it can be recognized after an approximately 3.3-nm-thick pentacene layer is deposited. The clear observation and energy-level identification of the pentacene HOMO level occurs for a pentacene layer with an estimated thickness of 5.8 nm, at which point all the pentacene valence region features are resolved. The location of HOMO onset of pentacene is 0.73 eV lower than the Fermi level of Au. Figure 1(b) shows the work function of the deposited pentacene films as a function of film thickness, extracted from the secondary electron cutoff. Upon pentacene deposition, the work function decreases and quickly stabilizes at around 4.3 eV. A large interface dipole with magnitude of 0.95 eV is measured at the interface of pentacene and polycrystalline gold. The corresponding dia-

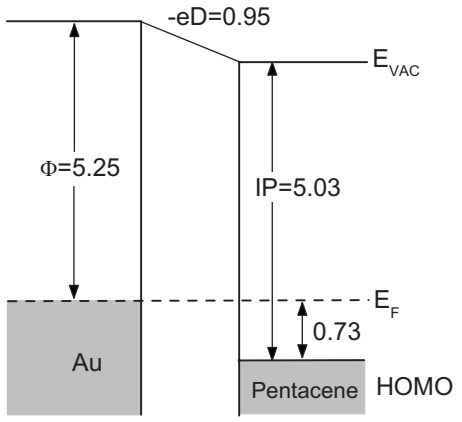


FIG. 2. Energy diagram of the interfaces between pentacene and polycrystalline Au with eD standing for interface dipole, and $E_{VAC}$ presenting the vacuum level. All energy values are expressed in eV.

gram of energy-level alignment between pentacene and Au extracted from the UPS data is summarized in Fig. 2. Note that the formation of pentacene film on polycrystalline Au substrate is more complicated than layer-by-layer growth as evident from the 5.8-nm thickness necessary to achieve ~full coverage (saturation of the pentacene UPS features) as well as from previous studies.[41,51,52] The orientation of pentacene on polycrystalline surfaces is very complicated, which results in a variation in the vertical ionization potential (IP) of pentacene film between 4.7 to 5.3 eV.[53]

### B. Pentacene on 1 ML $C_{60}$/Au foil

As noted, due to the complexity of pentacene molecular orientation on a polycrystalline Au surface, a variation in hole-injection barriers and IPs can be expected. This, in turn, is expected to affect turn on voltage and hole currents in devices. Hence, more reproducible film growth in terms of pentacene orientation at the interface is desired in order to achieve devices with better and more reproducible performance. On the other hand, the orientation of initial pentacene monolayer and the following molecular order strongly depends upon the electronic interaction between $\pi$ orbitals of pentacene and empty $d$ orbitals of the metal atoms, where charge-transfer and substrate-adsorbate interaction can dominate the process. To control the molecular orientation of pentacene, the key issue is to modify/decouple the influence of metal surface. One approach to this issue is to adsorb an organic monolayer on metal surface, which allows not only for controlling the orientation of pentacene layer but also for tuning the electronic interaction between pentacene and metal surface. It has been recently suggested that the long-range order in molecular adsorption on metal surfaces can be modified by choosing a noninteracting buffer layer for decoupling the influence of the metal, driving a weak interaction between pentacene single-layer and metal surfaces.[54,55] Here we pursue this route, tuning the pentacene orientation by modifying the interface charge transfer, using $C_{60}$ molecules as an interfacial monolayer. $C_{60}$ was chosen as it has no spatial orientation at room temperature and the preparation of monolayer films is well-known. Furthermore, due to

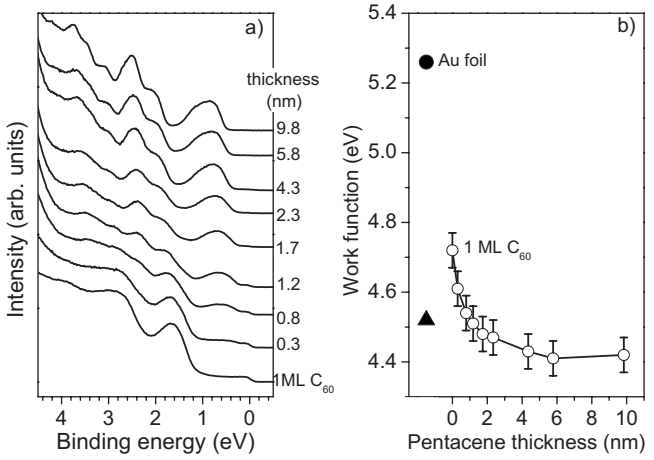


FIG. 3. (a) Evolution of UPS spectra of pentacene on 1 ML $C_{60}$/Au with increasing pentacene thickness. (b) The variation in work function as a function of pentacene film thickness adsorbed on 1 ML $C_{60}$/Au. For comparison, the work-function value of Au foil (full circle) and thick $C_{60}$ (full triangle) also shown together.

the high electron affinity of $C_{60}$, charge transfer from metal substrate to $C_{60}$ is often observed, which leads to the formation of an interfacial dipole layer.

Figure 3 contains the UPS valence-band spectra of pentacene film grown on 1 ML $C_{60}$ on polycrystalline gold surface. The well-known spectral feature of monolayer $C_{60}$ is shown in the bottom curve. Due to electron charge transfer from Au to $C_{60}$, the states in the vicinity of the Fermi edge are ascribed to the partially filled lowest unoccupied molecular orbitals of $C_{60}$ and density of states coming from Au metal.[48,49] The HOMO onset of the monolayer $C_{60}$ is situated at 1.15 eV below the Fermi level which is about 0.8 eV lower than that of thick $C_{60}$ film. Upon incremental deposition of the pentacene overlayer, the $C_{60}$ spectral feature is quickly suppressed. At a pentacene film thickness of 1.2 nm, the pentacene features have been well developed and the $C_{60}$ signal almost disappears. At 1.7 nm, the pentacene features are fully developed, and the Fermi edge is completely suppressed. This is in sharp contrast to the case of pentacene adsorbed directly on a polycrystalline Au substrate, where the Au signal is still present for the 3.2-nm pentacene overlayer spectrum and the Fermi edge is still visible even at 5.8-nm-thick pentacene films, both indicative of island growth mechanism.[41,44,51,52] A significantly more uniform growth of pentacene films is hence achieved with the 1 ML $C_{60}$ interfacial layer. It should be mentioned that there is a feature in the UPS spectrum at around 2 eV, observed for the thick pentacene film, which is present in proximity to the $C_{60}$ HOMO peak. The pentacene-originated contribution is related to the $2a_{2u}$ (HOMO-1) molecular state.[56] From the evolution of the peak intensity around 2 eV, it can be clearly seen that the $C_{60}$ HOMO peak is suppressed with increasing pentacene coverage. It reaches minimum at 1.7 nm pentacene (monolayer coverage), after that the pentacene HOMO-1 peak intensity increases with pentacene coverage. Considering the molecular size of pentacene, it is a planar molecule consisting of five benzene rings linearly linked, with a size of 1.5 nm along long axis, 0.6 nm in the short

axis, the saturation of spectral feature reached at 1.7-nm film thickness is indicative of ~full film coverage with one monolayer of pentacene. The evolution of the work function upon increased pentacene deposition onto the monolayer $C_{60}$/Au substrate is shown in Fig. 3(b). The work function of clean Au substrate is 5.23 eV. Upon deposition of thick $C_{60}$ film followed by a high-temperature annealing step, the stronger interaction between $C_{60}$ and Au than $C_{60}$-$C_{60}$ produces a uniform monolayer $C_{60}$, where the amount of charge transfer is about 1.0 electron per $C_{60}$ molecule on Au substrate, the effective work function of gold with monolayer $C_{60}$ is about 4.7 eV. Deposition of pentacene leads to a continuous decrease in the substrate work function, which saturates at about 4.4 eV. Already for 2-nm-thick pentacene films, the work function is close to saturation, which is consistent with the full development of UPS valence-band spectral features and ~full coverage of pentacene on the $C_{60}$/Au surface. The evolution of the C 1*s* XPS spectra also confirms such saturation (data not shown). With increasing pentacene thickness, the C 1*s* peak slowly downshifts and reaches to 283.85 eV, whereas the C 1*s* peak position of monolayer $C_{60}$ is at 284.35 eV. (The exact position of pentacene peak at the early stage of film formation is not resolved in the C 1*s* spectrum). The downshift in the C 1*s* peak position stops after the pentacene thickness reaches 1.7 nm, i.e., upon further deposition no shift in the C 1*s* peak position is observed. In view of the UPS and C 1*s* XPS data all saturating at 1.7 nm, and considering the pentacene size and spherical shape of $C_{60}$, we concluded that pentacene molecules form a monolayer on $C_{60}$ upon vacuum deposition with their long axis parallel to the surface normal rather than having a flat orientation on the monolayer of $C_{60}$. As already discussed, modifying the charge transfer at an organic-metal interface may affect long-range molecular order and hence growth mechanism. Furthermore, pentacene has a stronger intermolecular interaction with a parallel geometry due to the $\pi-\pi$ bonding interaction. Although the $C_{60}$ molecule also has a $\pi$-bonding structure, the curvature effect of the $C_{60}$ ball will reduce the $\pi-\pi$ interaction with a pentacene lying on top. Pentacene molecules lying flat on $C_{60}$ is therefore expected to be an energetically unfavorable ordering scheme as compared to pentacene molecules standing up at the pentacene/$C_{60}$ interface. In contrast, for a highly ordered pyrolytic graphite (HOPG) surface, which is flat unlike the curved $C_{60}$, pentacene is deposited with a flat orientation as this will maximize $\pi-\pi$ interaction between the graphene layer and the pentacene plane.[57] On the other hand, in the case of pentacene deposited on clean metal surface, the strong influence of the bare metal surface on molecular overlap and state mixing cannot be neglected.[58] Hybridization between the $\pi$-molecular orbitals with metal states can give rise to mixed metal-pentacene orbitals delocalized over the interface region. The presence of the fullerene buffer layer can actually break the strong coupling between pentacene and the bare metal surface, which leads to modification of the electronic and structural properties of the absorbed pentacene film. As a result, an upright standing pentacene molecular layer is achieved.

The hole-injection barrier into pentacene is a crucial parameter in pentacene-based device performance. For the clean Au substrate, the difference between the Fermi level and the IP of the pentacene film is about 0.73 eV, as shown in Fig. 2. Figure 3(a) clearly demonstrates that this difference is decreased significantly for pentacene films on 1 ML $C_{60}$/Au film, to about 0.26 eV at a pentacene film thickness of 1.7 nm (~monolayer of pentacene). The $E_F$ vs IP difference is increased slightly for thick pentacene films, probably due to polarization effects.[42,44,59] The difference is ~0.4 eV at thick films, still far lower than that for the case of the unmodified pentacene/Au contact. Since the energetics at the interfacial region is the most important for hole injection, the $C_{60}$ monolayer should have a strong influence on the hole-injection properties into pentacene. We have performed the same experiment on Ag substrates, where the $E_F$ vs IP difference at the pentacene interface is reduced from 1.1 eV for Ag substrates to 0.4 eV for the modified 1 ML $C_{60}$/Ag substrate, further evidence of the utility of adsorbing one monolayer $C_{60}$ molecules on metal surfaces to improve hole injection into pentacene (and other hole-transporting materials).

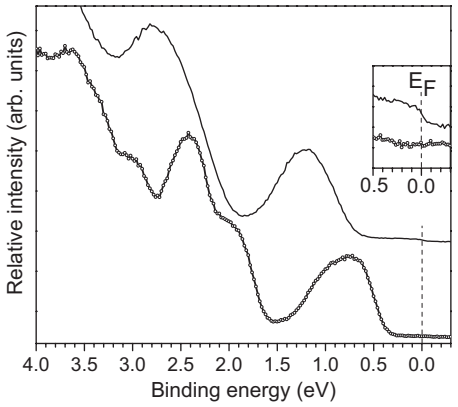


FIG. 4. Comparison between UPS spectra of pentacene at a nominal film thickness of 5.8 nm on polycrystalline gold (solid line, top) and on 1 ML $C_{60}$ modified Au (open-circle-line, bottom), respectively. The dashed line represents the position of the Fermi edge. The inset indicates the enlarged spectra around the Fermi edge, where the Fermi edge is still observable for 5.8-nm pentacene/Au, but it is completely suppressed for 5.8-nm pentacene/1 ML $C_{60}$/Au.

The UPS valence-band spectra of 5.8-nm-thick pentacene films on pure Au (top) and on 1 ML $C_{60}$-modified Au (bottom) are shown together in Fig. 4. As noted earlier for the pentacene-on-Au case, the photoemission signal from Fermi edge of Au is not yet completely suppressed even at 5.8-nm thickness due to the island growth mechanism of this system. Furthermore, the spectrum of pentacene-on-Au is broadened as compared to pentacene on 1 ML $C_{60}$-modified Au. For example, the two features around 2 and 2.5 eV of pentacene on 1 ML $C_{60}$-modified Au only correspond to a wide featureless peak around 2.8 eV for pentacene/Au. On the other hand, the lowest binding-energy peak in the valence band also manifests differences between the two systems. The symmetric HOMO peak of pentacene is observed in the pentacene/Au case, whereas the corresponding HOMO peak of pentacene on 1 ML $C_{60}$-modified Au substrate shows an asymmetric structure. The double-HOMO line shape in the latter case is due to the pentacene film with molecules stand-

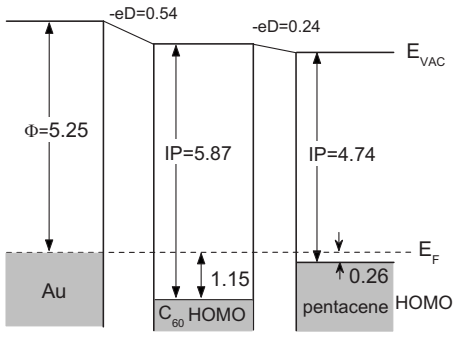


FIG. 5. Schematic energy-level diagram of pentacene on 1 ML $C_{60}$/polycrystalline gold with eD standing for interface dipole, and $E_{VAC}$ representing the vacuum level. All energy values are expressed in eV.

ing upright on the surface.[57] Compared with the HOMO peak splitting of pentacene on CuPc/HOPG,[57] the current double-HOMO feature is relatively weaker. A plausible explanation for the difference in the shape of HOMO feature is the rough surface of the 1 ML $C_{60}$-modified Au surface compared to the flat CuPc/HOPG. However, the data from pentacene film, adsorbed on metal crystal surface modified with self-assembled monolayer, indicate the similar weak double-HOMO lineshape.[55] So the weak splitting of the HOMO peak can be more likely ascribed to the typical arrangement of pentacene in quasibulklike fashion rather than the rough surface.

Based on the UPS data, an energy-level diagram of pentacene on 1 ML $C_{60}$/Au can be obtained, as shown in Fig. 5. The stronger dipole is between $C_{60}$ and Au: about 0.54 eV (push-back effect and charge transfer). The size of interface dipole between $C_{60}$ and pentacene is about 0.24 eV, which is slightly larger than dipole between pentacene and a thick $C_{60}$ film,[60] possibly due to polarization effects from the gold substrate. The total interface dipole between Au and pentacene is 0.78 eV, which is 0.2 eV smaller than pentacene on pure Au surface. Another significant difference between the two systems is the decrease in IP. For the 1 ML $C_{60}$/Au case, the pentacene IP is significantly lower, about 4.74 eV, which is in good agreement with the reported value for pentacene films in a crystalline phase consisting of upright standing molecules.[24,57] It should be mentioned that the decrease in IP value, for upright standing molecular orientation, was also observed for sexithiophene molecular layer, as compared to that with a flat-lying geometry. The applied theoretical model revealed the presence of an intrinsic surface dipole in the ordered molecular layer, which modifies IP value of about 0.5 eV.[27] Further theoretical studies on the ordered pentacene molecular layer could bring more insight in this effect and allow for estimation of the upper limit of the variations in IP values for various pentacene films. On the other hand, the variation in IP also has important implications for organic electronic applications. Due to smaller size of the interface dipole and the lower IP in the pentacene film, a significant decrease in the hole-injection barrier of the ordered pentacene film is achieved, which should improve device performance. Recent measurements related to organic transistors further confirm such improvement. A pentacene-based thin-film transistor with UV/ozone treated Au electrodes demonstrates a significant decrease in hole-injection barrier, improved morphology of pentacene film, and orders-of-magnitude reduction in the contact resistance.[61]

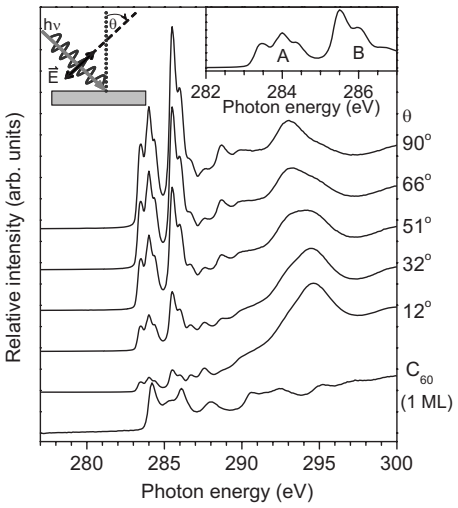


FIG. 6. Carbon $K$ edge x-ray absorption spectra of the pentacene film on 1 ML $C_{60}$-modified Au substrate with different incident angles. The angle, $\theta$, is the polar angle between the electric vector field of the incident x-ray beam and the substrate surface normal, as shown in top-left figure, where the normal incidence corresponds to $\theta=90°$. Inset shows the lowest energy adsorption features A and B at $\theta=66°$. For comparison, the C $K$-edge absorption spectra of 1 ML $C_{60}$/Au was shown in the bottom curve.

### C. Polarized x-ray absorption of pentacene on 1 ML $C_{60}$/Au

To further confirm the molecular orientation of pentacene on 1 ML $C_{60}$/Au surfaces, polarized x-ray absorption was performed, where the excitation from the C 1$s$ core level (C $K$ edge) into the unoccupied electronic states of a pentacene film can be probed. Due to a flat $sp^2$ hybridized carbon system in pentacene, C 1$s$ core-level excitations into $\pi^*$-derived molecular states are only possible for a polarization of the synchrotron light perpendicular to the molecular plane, while those into states with $\sigma^*$ character are seen for light polarization within the molecular planes.[62]

Figure 6 represents the polarization angle dependent x-ray absorption spectra of a pentacene overlayer film (approximately five monolayers) deposited on 1 ML $C_{60}$-modified polycrystalline gold, where the bottom line indicates the absorption spectrum of 1 ML $C_{60}$ on Au. For the absorption spectrum of the pentacene film at lower photon energy, there are two components clearly resolved in the spectrum, marked as A and B in the inset of Fig. 6, which arise from excitations into $\pi^*$ orbitals of the molecular system, the so-called $\pi^*$ resonances.[63] In detail, several separate components in an energy region between 283 and 286.5 eV can be identified.[64] These features have out-of-plane character and are used in the following to evaluate the intensity of the $\pi^*$ resonances. Although the spectral features result from the transitions from C 1$s$ core level to unoccupied molecular states, the features do not represent the energy positions of the unoccupied

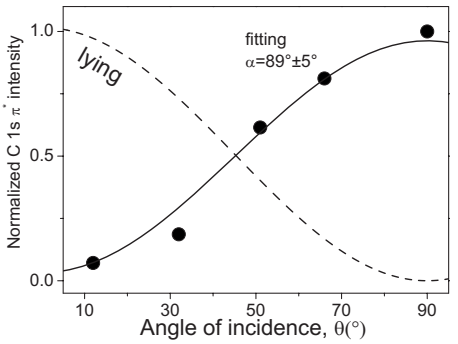


FIG. 7. Angle dependence of the $\pi^*$ resonance intensity of pentacene on 1 ML $C_{60}$/Au (full circle). The solid line is the result of the fitting process, which produces pentacene molecules almost vertically standing on the surface at a degree of $89° \pm 5°$ to the substrate surface. The dashed line simulates the C $1s$ $\pi^*$ intensity distribution of pentacene film at a perfect lying geometry under the current experimental condition.

density of states due to excitonic effects involving the core hole.[65,66] The energetically lowest lying feature can be assigned unambiguously to excitations into the lowest unoccupied molecular orbital of pentacene, however.

The significant feature of Fig. 6 is that the intensity of the C $1s$ to $\pi^*$ transition changes with the incidence angle of the photon beam. The highest intensity is seen for close to normal incidence, whereas the intensity at grazing incidence is comparatively small. The intensity of the C $1s$ to $\pi^*$ excitations is summarized in Fig. 7 as a function of the polarization angle. Furthermore, taking into account the 95% linear polarization of the synchrotron radiation, the inclination angle of the pentacene film deposited on 1 ML $C_{60}$/Au could be extracted, which yielded an angle of $89° \pm 5°$ with respect to the surface.[62,67] The experimental results give an evidence that the pentacene molecules were adsorbed on the surface in a nearly vertical standing-up geometry.

With x-ray absorption one can only determine the orientation of the electronic $\pi$ orbitals of the molecules in the organic overlayers. For pentacene on 1 ML $C_{60}$/Au substrate, these orbitals are directed parallel to the surface, i.e., the molecular plane is parallel to the surface normal. From the absorption data we hence cannot judge if the pentacene molecules are standing on their long or their short side. The photoelectron spectroscopy data, where the saturation of work function and peak positions is found at about 1.7 nm of nominal film thickness, suggests that pentacene molecules are standing with their long axis parallel to surface normal. For the ordering case of the short axis parallel to surface normal, saturation should have been reached at roughly half of this thickness, which is clearly not the case. We can conclude that when deposited onto $C_{60}$-modified polycrystalline gold, pentacene molecules will stand on the surface with their long axis parallel to the surface normal. The standing geometry will enhance the intramolecular interaction and provide a reliably ordered interface, which should be beneficial for device applications.

## IV. CONCLUSIONS

In summary, we have studied the electronic properties of pentacene film deposition on a monolayer $C_{60}$-modified polycrystalline gold surface by photoemission and polarized x-ray absorption spectroscopy. The adsorption of monolayer $C_{60}$ tunes the pentacene growth mechanism, influencing the corresponding electronic properties of the interface. The island growth of pentacene with randomly orientated molecules on pure metal surfaces is overcome by inserting the $C_{60}$ monolayer, producing an interface where pentacene molecules form a standing-up orientation with their long axis parallel to the surface normal. The $C_{60}$ monolayer presents a novel interface modification that reduces the size of the interface dipole between pentacene and the Au surface. The hole-injection barrier into the pentacene films is significantly lowered as is the IP value as compared to pentacene-on-Au interface. The induced orientation leads to a stronger $\pi-\pi$ overlap between the pentacene molecules that will likely enhance the transport properties in corresponding devices.

## ACKNOWLEDGMENTS

The research leading to these results has received funding from the European Community's Seventh Framework Programme (FP7/2007-2013) under Grant Agreement No. 212311 of the ONE-P project. The authors acknowledge financial support from the Swedish Research Council (project grant, and Linneus center) and the Knut and Alice Wallenberg Foundation.

[1] J. Birgerson, K. Kaeriyama, P. Barta, P. Bröms, M. Fahlman, T. Granlund, and W. R. Salaneck, Adv. Mater. **8**, 982 (1996).
[2] N. S. Sariciftci, L. Smilowitz, A. J. Heeger, and F. Wudl, Science **258**, 1474 (1992).
[3] F. Garnier, R. Hajlaoui, A. Yassar, and P. Srivastava, Science **265**, 1684 (1994).
[4] P. W. M. Blom, M. J. M. de Jong, and C. T. H. F. Liedenbaum, Polym. Adv. Technol. **9**, 390 (1998).
[5] A. C. Morteani, P. Sreearunothai, L. M. Herz, R. H. Friend, and C. Silva, Phys. Rev. Lett. **92**, 247402 (2004).
[6] L. J. A. Koster, V. D. Mihailetchi, and P. W. M. Blom, Appl. Phys. Lett. **88**, 093511 (2006).
[7] H. Ishii, K. Sugiyama, E. Ito, and K. Seki, Adv. Mater. **11**, 605 (1999).
[8] S. Braun, W. R. Salaneck, and M. Fahlman, Adv. Mater. **21**, 1450 (2009).
[9] J. Hwang, A. Wan, and A. Kahn, Mat. Sci. Eng. R. **64**, 1 (2009).
[10] X. Crispin, V. M. Geskin, A. Crispin, J. Cornil, R. Lazzaroni, W. R. Salaneck, and J. L. Brédas, J. Am. Chem. Soc. **124**, 8131 (2002).
[11] A. Kahn, N. Koch, and W. Y. Gao, J. Polym. Sci., Part B: Polym. Phys. **41**, 2529 (2003).
[12] M. Knupfer and H. Peisert, Phys. Status Solidi A **201**, 1055 (2004).

[13] W. R. Salaneck and M. Fahlman, J. Mater. Res. **19**, 1917 (2004).
[14] M. Fahlman, A. Crispin, X. Crispin, S. K. M. Henze, M. P. de Jong, W. Osikowicz, C. Tengstedt, and W. R. Salaneck, J. Phys.: Condens. Matter **19**, 183202 (2007).
[15] H. Fukagawa, S. Kera, T. Kataoka, S. Hosoumi, Y. Watanabe, K. Kudo, and N. Ueno, Adv. Mater. **19**, 665 (2007).
[16] S. Braun and W. R. Salaneck, Chem. Phys. Lett. **438**, 259 (2007).
[17] G. Heimel, L. Romaner, E. Zojer, and J. L. Bredas, Acc. Chem. Res. **41**, 721 (2008).
[18] N. Koch, J. Phys.: Condens. Matter **20**, 184008 (2008).
[19] G. Greczynski, M. Fahlman, and W. R. Salaneck, Chem. Phys. Lett. **321**, 379 (2000).
[20] C. Tengstedt, W. Osikowicz, W. R. Salaneck, I. D. Parker, C.-H. Hsu, and M. Fahlman, Appl. Phys. Lett. **88**, 053502 (2006).
[21] S. Braun, W. Osikowicz, Y. Wang, and W. R. Salaneck, Org. Electron. **8**, 14 (2007).
[22] S. Braun, M. P. de Jong, W. Osikowicz, and W. R. Salaneck, Appl. Phys. Lett. **91**, 202108 (2007).
[23] H. Vázquez, Y. J. Dappe, J. Ortega, and F. Flores, Appl. Surf. Sci. **254**, 378 (2007).
[24] M. G. Betti, A. Kanjilal, C. Mariani, H. Vazquez, Y. J. Dappe, J. Ortega, and F. Flores, Phys. Rev. Lett. **100**, 027601 (2008).
[25] W. Osikowicz, M. P. de Jong, S. Braun, C. Tengstedt, M. Fahlman, and W. R. Salaneck, Appl. Phys. Lett. **88**, 193504 (2006).
[26] G. Heimel, L. Romaner, J. L. Brédas, and E. Zojer, Phys. Rev. Lett. **96**, 196806 (2006).
[27] S. Duhm, G. Heimel, I. Salzmann, H. Glowatzki, R. L. Johnson, A. Vollmer, J. P. Rabe, and N. Koch, Nature Mater. **7**, 326 (2008).
[28] I. Salzmann, S. Duhm, G. Heimel, M. Oehzelt, R. Kniprath, R. L. Johnson, J. P. Rabe, and N. Koch, J. Am. Chem. Soc. **130**, 12870 (2008).
[29] Y.-E. Kim, H. Park, and J.-J. Kim, Appl. Phys. Lett. **69**, 599 (1996).
[30] F. Li, H. Tang, J. Anderegg, and J. Shinar, Appl. Phys. Lett. **70**, 1233 (1997).
[31] G. Greczynski, M. Fahlman, and W. R. Salaneck, J. Chem. Phys. **113**, 2407 (2000).
[32] Y. Q. Zhan, X. J. Liu, E. Carlegrim, F. H. Li, I. Bergenti, P. Graziosi, V. Dediu, and M. Fahlman, Appl. Phys. Lett. **94**, 053301 (2009).
[33] W. Osikowicz, X. Crispin, C. Tengstedt, L. Lindell, T. Kugler, and W. R. Salaneck, Appl. Phys. Lett. **85**, 1616 (2004).
[34] N. Koch, S. Duhm, J. Rabe, S. Rentenberger, R. Johnson, J. Klankermayer, and F. Schreiber, Appl. Phys. Lett. **87**, 101905 (2005).
[35] N. Koch, S. Duhm, J. P. Rabe, A. Vollmer, and R. L. Johnson, Phys. Rev. Lett. **95**, 237601 (2005).
[36] F. L. E. Jakobsson, X. Crispin, L. Lindell, A. Kanciurzewska, M. Fahlman, W. R. Salaneck, and M. Berggren, Chem. Phys. Lett. **433**, 110 (2006).
[37] L. Lindell, M. Unge, W. Osikowicz, S. Stafström, W. R. Salaneck, X. Crispin, and M. P. de Jong, Appl. Phys. Lett. **92**, 163302 (2008).
[38] K. Itaka, M. Yamashiro, J. Yamaguchi, M. Haemori, S. Yaginuma, Y. Matsumoto, M. Kondo, and H. Koinuma, Adv. Mater. **18**, 1713 (2006).
[39] S. Lee, B. Koo, J. Shin, E. Lee, H. Park, and H. Kim, Appl. Phys. Lett. **88**, 162109 (2006).
[40] J. Yang and T. Q. Nguyen, Org. Electron. **8**, 566 (2007).
[41] R. Ruiz, D. Choudhary, B. Nickel, T. Toccoli, K. Chang, A. C. Mayer, P. Clancy, J. M. Blakely, R. L. Headrick, S. Iannotta, and G. Malliaras, Chem. Mater. **16**, 4497 (2004).
[42] F. Amy, C. Chan, and A. Kahn, Org. Electron. **6**, 85 (2005).
[43] K. Ihm, B. Kim, T. H. Kang, K. J. Kim, M. H. Joo, T. H. Kim, S. S. Yoon, and S. Chung, Appl. Phys. Lett. **89**, 033504 (2006).
[44] N. Koch, A. Kahn, J. Ghijsen, J. J. Pireaux, J. Schwartz, R. L. Johnson, and A. Elschner, Appl. Phys. Lett. **82**, 70 (2003).
[45] N. J. Watkins, L. Yan, and Y. L. Gao, Appl. Phys. Lett. **80**, 4384 (2002).
[46] H. Peisert, T. Schwieger, M. Knupfer, M. S. Golden, and J. Fink, J. Appl. Phys. **88**, 1535 (2000).
[47] M. P. Seah and W. A. Dench, Surf. Interface Anal. **1**, 2 (1979).
[48] B. W. Hoogenboom, R. Hesper, L. H. Tjeng, and G. A. Sawatzky, Phys. Rev. B **57**, 11939 (1998).
[49] L. H. Tjeng, R. Hesper, A. C. L. Heessels, A. Heeres, H. T. Jonkman, and G. A. Sawatzky, Solid State Commun. **103**, 31 (1997).
[50] T. R. Ohno, Y. Chen, S. E. Harvey, G. H. Kroll, J. H. Weaver, R. E. Haufler, and R. E. Smalley, Phys. Rev. B **44**, 13747 (1991).
[51] D. Kafer, L. Ruppel, and G. Witte, Phys. Rev. B **75**, 085309 (2007).
[52] Y. Zheng, D. C. Qi, N. Chandrasekhar, X. Y. Gao, C. Troadec, and A. T. S. Wee, Langmuir **23**, 8336 (2007).
[53] N. Sato, K. Seki, H. Inokuchi, and Y. Harada, Chem. Phys. **109**, 157 (1986).
[54] W. S. Hu, Y. T. Tao, Y. J. Hsu, D. H. Wei, and Y. S. Wu, Langmuir **21**, 2260 (2005).
[55] M. G. Betti, A. Kanjilal, and C. Mariani, J. Phys. Chem. A **111**, 12454 (2007).
[56] C. Baldacchini, C. Mariani, M. G. Betti, L. Gavioli, M. Fanetti, and M. Sancrotti, Appl. Phys. Lett. **89**, 152119 (2006).
[57] H. Fukagawa, H. Yamane, T. Kataoka, S. Kera, M. Nakamura, K. Kudo, and N. Ueno, Phys. Rev. B **73**, 245310 (2006).
[58] A. Ferretti, C. Baldacchini, A. Calzolari, R. Di Felice, A. Ruini, E. Molinari, and M. G. Betti, Phys. Rev. Lett. **99**, 046802 (2007).
[59] H. Peisert, M. Knupfer, T. Schwieger, J. M. Auerhammer, M. S. Golden, and J. Fink, J. Appl. Phys. **91**, 4872 (2002).
[60] S. J. Kang, Y. Yi, C. Y. Kim, S. W. Cho, M. Noh, K. Jeong, and C. N. Whang, Synth. Met. **156**, 32 (2006).
[61] B. Stadlober, U. Haas, H. Gold, A. Haase, G. Jakopic, G. Leising, N. Koch, S. Rentenberger, and E. Zojer, Adv. Funct. Mater. **17**, 2687 (2007).
[62] J. Stöhr, *NEXAFS Spectroscopy* (Springer, Berlin, 1992).
[63] M. Alagia, C. Baldacchini, M. G. Betti, F. Bussolotti, V. Carravetta, U. Ekstrom, C. Mariani, and S. Stranges, J. Chem. Phys. **122**, 124305 (2005).
[64] T. Schwieger, X. Liu, D. Olligs, M. Knupfer, and T. Schmidt, J. Appl. Phys. **96**, 5596 (2004).
[65] P. A. Bruhwiler, A. J. Maxwell, C. Puglia, A. Nilsson, S. Andersson, and N. Martensson, Phys. Rev. Lett. **74**, 614 (1995).
[66] E. J. Mele and J. J. Ritsko, Phys. Rev. Lett. **43**, 68 (1979).
[67] M. Chiodi, L. Gavioli, M. Beccari, V. Di Castro, A. Cossaro, L. Floreano, A. Morgante, A. Kanjilal, C. Mariani, and M. G. Betti, Phys. Rev. B **77**, 115321 (2008).